Supplementary Material:

Polyamine induced tannic acid co-deposition on magnetic nanoparticles for enzyme immobilization and its efficient biodiesel production under alternating magnetic field

Wen Tang[a], Tonghao Ma[b], Lina Zhou[b], Gaoya Wang[a], Xiaoli Wang[b], Hanjie Ying[c], Chao Chen[b,*], Ping Wang[d]

[a]State Key Laboratory of Bioreactor Engineering, New World Institute of Biotechnology, East China University of Science and Technology, No.130 Meilong Road, Shanghai 200237, People's Republic of China.

[b]State Key Laboratory of Bioreactor Engineering, Biomedical Nanotechnology Center, School of Biotechnology, East China University of Science and Technology, Shanghai 200237, People's Republic of China. E-mail addresses: chaochen@ecust.edu.cn.

[c]State Key Laboratory of Materials-Oriented Chemical Engineering, College of Biotechnology and Pharmaceutical Engineering, Nanjing Tech University, Puzhu South Road, Nanjing 211816, People's Republic of China.

[d]Department of Bioproducts and Biosystems Engineering, University of Minnesota, St Paul, MN 55108, USA.

Experiments:

FITC-labeled CALB

According to previous studies with slightly modification [1], Fluorescein isothiocyanate (FITC)-labeled CALB were prepared by adding 0.6 mL of FITC/DMSO solution (0.5 mg/mL) to 8 mL of CALB solution (0.5 mg/mL). After reaction for 1 h, the suspension was dialyzed against pH 7.0 PB for 72 h. Afterwards, FITC-labeled CALB were immobilized on Fe_3O_4-pTAPA nanoparticles and characterized by confocal laser scanning microscopy (CLSM).

Leakage experiment

The leakage experiment of immobilized CALB was conducted according to previous study with minor modification [2]. Specifically, 25 mg of Fe_3O_4-pTAPA-CALB and Fe_3O_4-pTA-CALB were incubated into 30 mL of PBS solution (20 mM, pH 7.0) with stirring rate of 250 rpm, respectively. After stirring for 7 days, the Fe_3O_4-pTAPA-CALB and Fe_3O_4-pTA-CALB were collected by a magnet. Meanwhile, the concentration of CALB in supernatant was measured by Bradfored method to determine the leakage profiles of enzyme from Fe_3O_4-pTAPA-CALB and Fe_3O_4-pTA-CALB. The enzyme leakage was calculated by the following equation:

$$\text{Enzyme leakage (\%)} = (C_i V_i)/M_0 \times 100$$

Where C_i represents the concentration of CALB released in the buffer solution, V_i is the buffer volume, and M_0 means the initial amount of immobilized CALB.

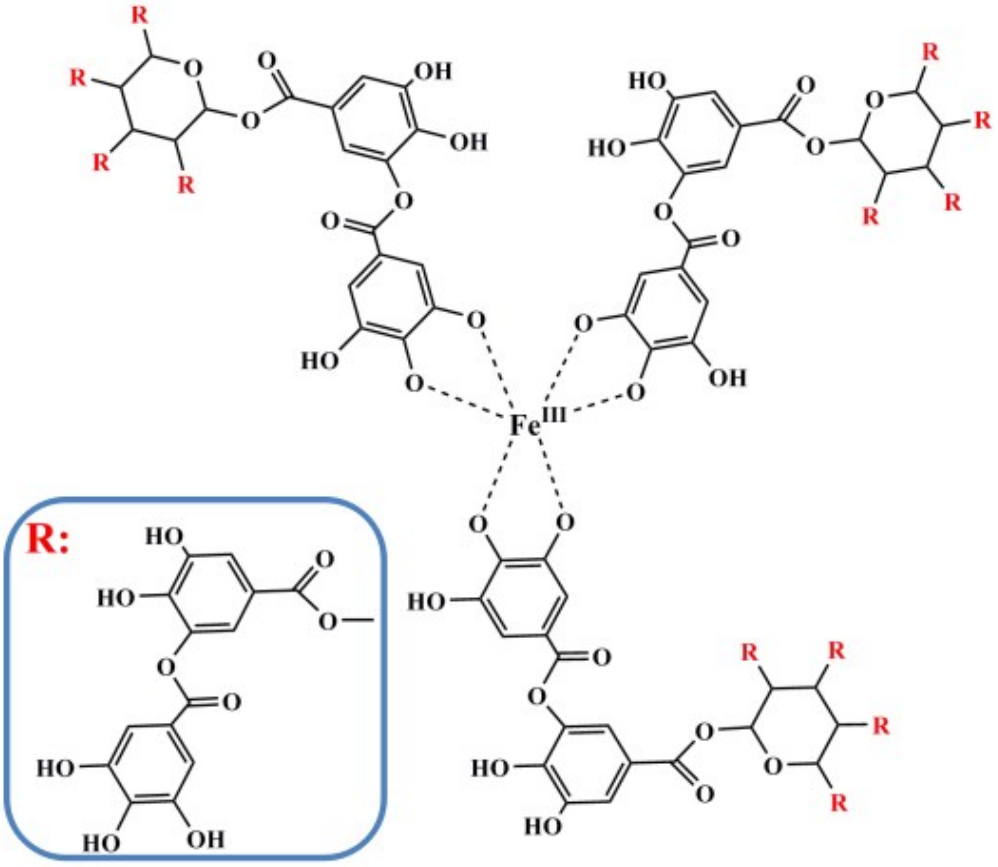

Fig. S1. The dominant Fe^{III}-TA complexation state in Fe_3O_4-pTAPA nanoparticles.

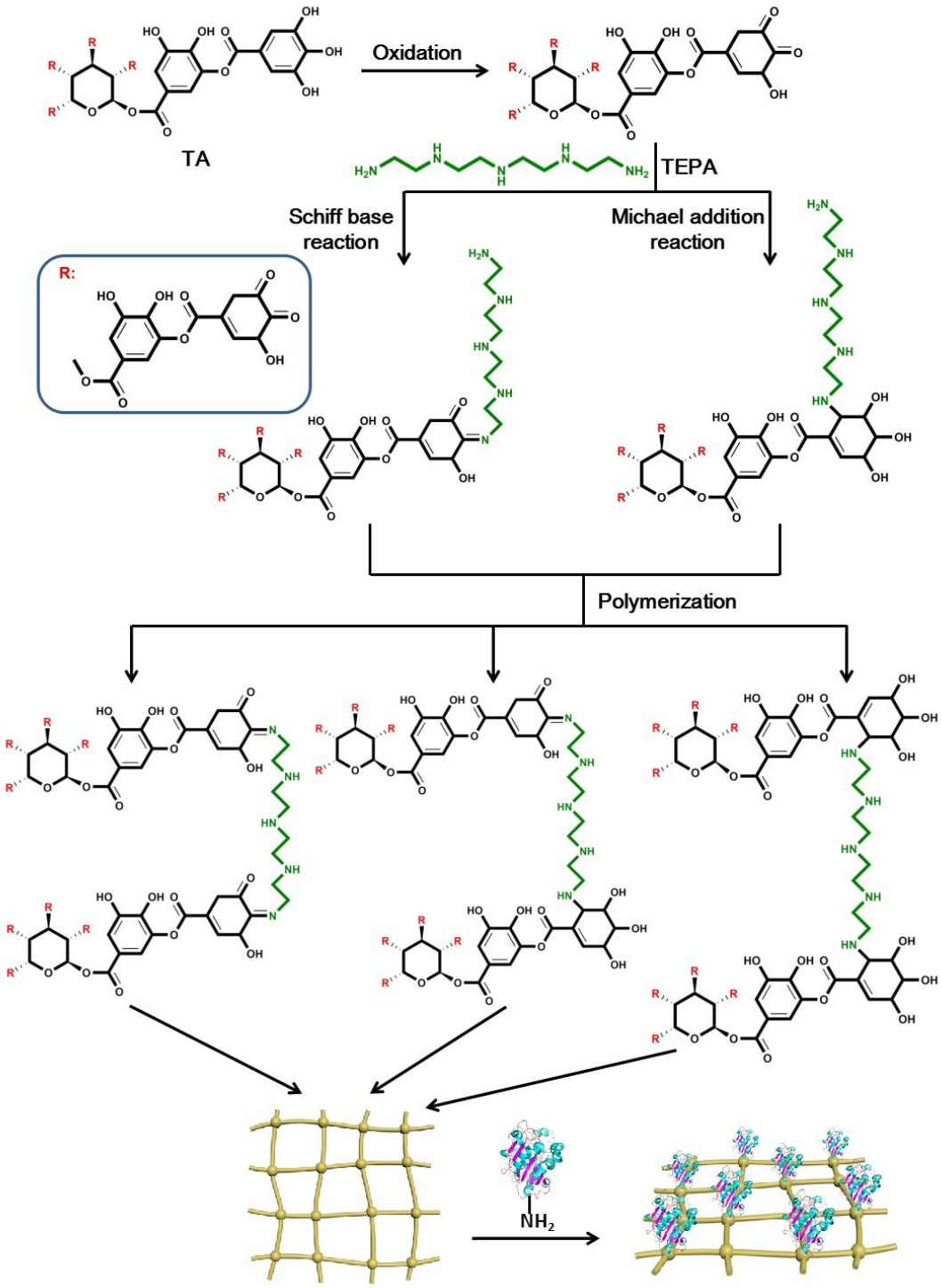

Fig. S2. The possible reaction mechanism for the forming of pTAPA layer and the covalent immobilization of CALB.

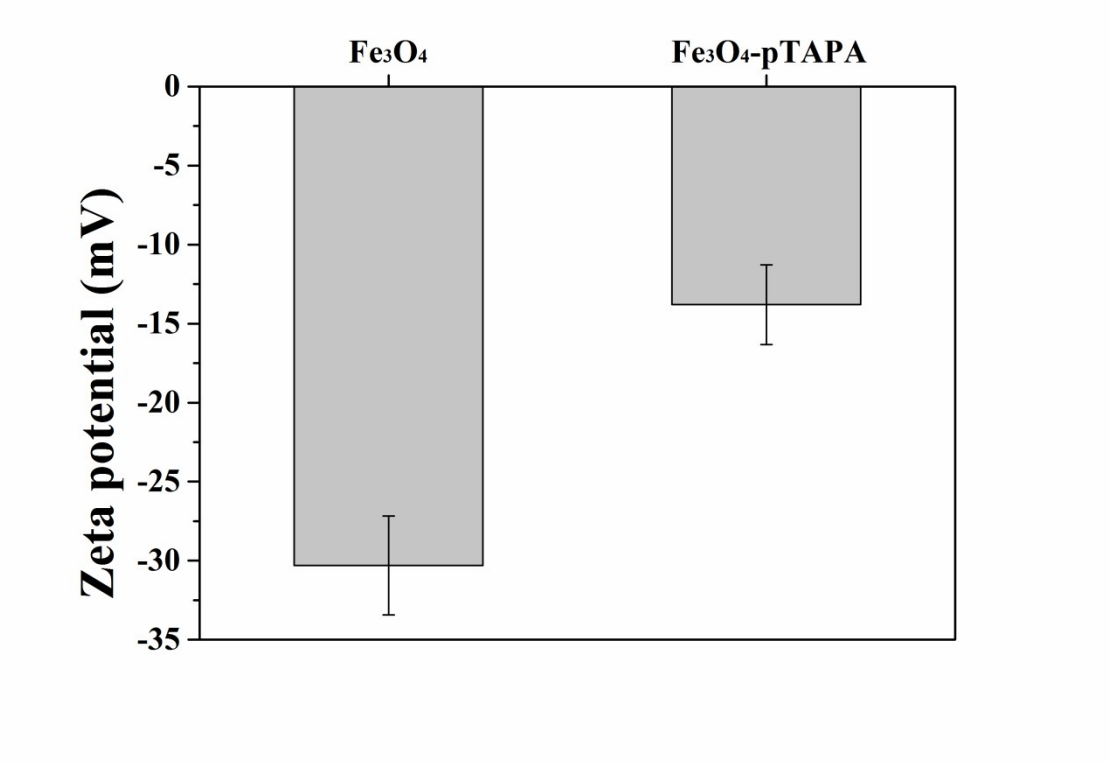

Fig. S3. Zeta potential of Fe_3O_4 and Fe_3O_4-pTAPA nanoparticles. Data are represented as mean ± SD (n = 3).

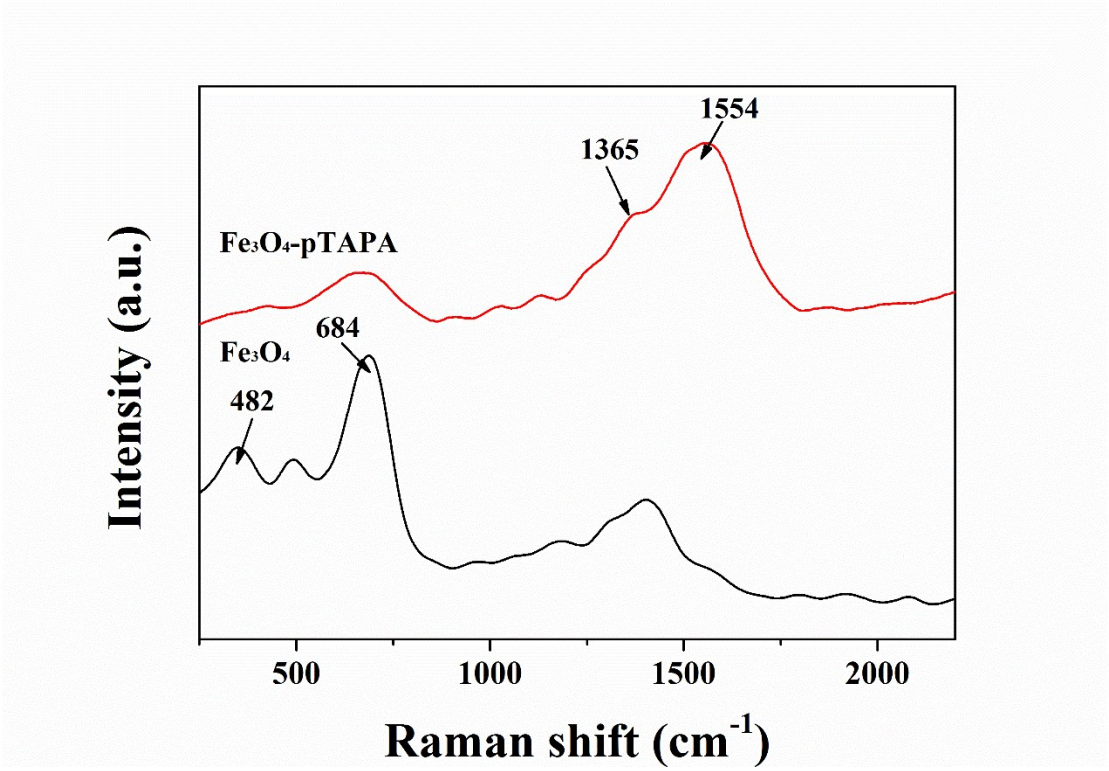

Fig. S4. Raman spectra of Fe_3O_4 and Fe_3O_4-pTAPA nanoparticles.

To evidently confirm the successfully modification of pTAPA layer on Fe_3O_4 nanoparticles, Raman spectroscopy was used in demonstrating the changes of the interface of Fe_3O_4-pTAPA nanoparticles. The Raman spectrum of bare Fe_3O_4 nanoparticles shows two strong bands around 482 and 684 cm^{-1}, which correspond to the T2g and A1g modes of symmetry[3]. However, after modification Fe_3O_4 nanoparticles with pTAPA layer, the intensity of these two characteristic bands decreased obviously, and two new broad characteristic bands around 1365 and 1554 cm^{-1} were present in the Raman spectrum of Fe_3O_4-pTAPA nanoparticles, which are attributed to the deformation of the catechol group in the pTAPA layer[3]. This result evidently confirmed the successful wrapping of pTAPA layer on Fe_3O_4 nanoparticles.

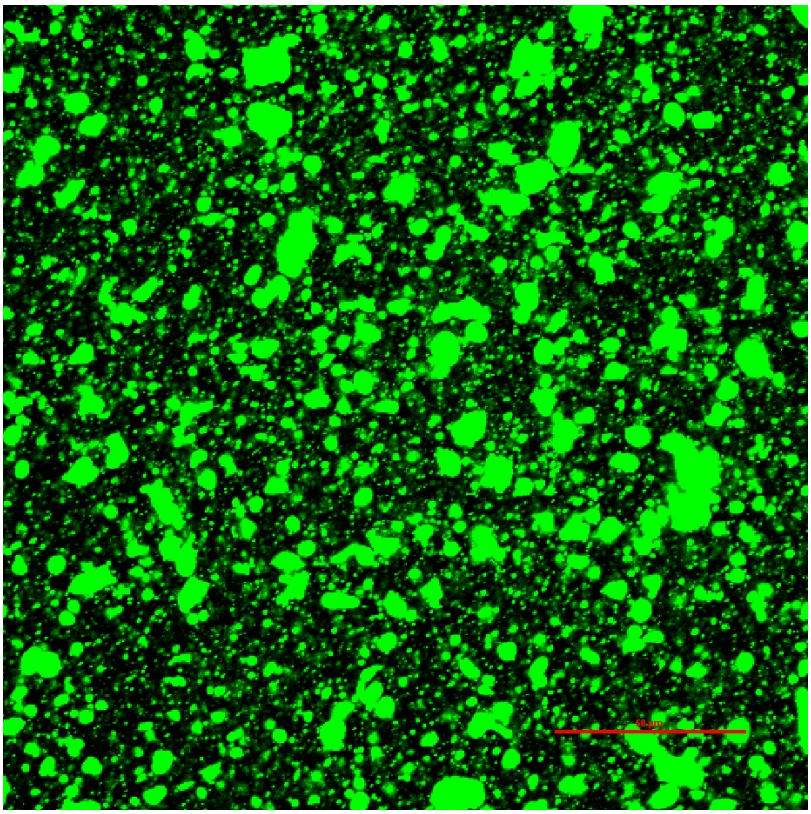

Fig. S5. The CLSM image of Fe_3O_4-pTAPA-CALB nanoparticles, and the CALB protein were labeled by FITC. Scale bar: 50 μm.

To directly indicate the CALB were successfully immobilized on the surface of Fe_3O_4-pTAPA nanoparticles, the Fe_3O_4-pTAPA-CALB nanoparticles was examined by CLSM. The fluorescence analysis of Fe_3O_4-pTAPA-CALB nanoparticles exhibited obviously green fluorescence due to the FITC-labeled CALB protein possessed of green fluorescence, demonstrating the CALB were indeed immobilized on Fe_3O_4-pTAPA nanoparticles.

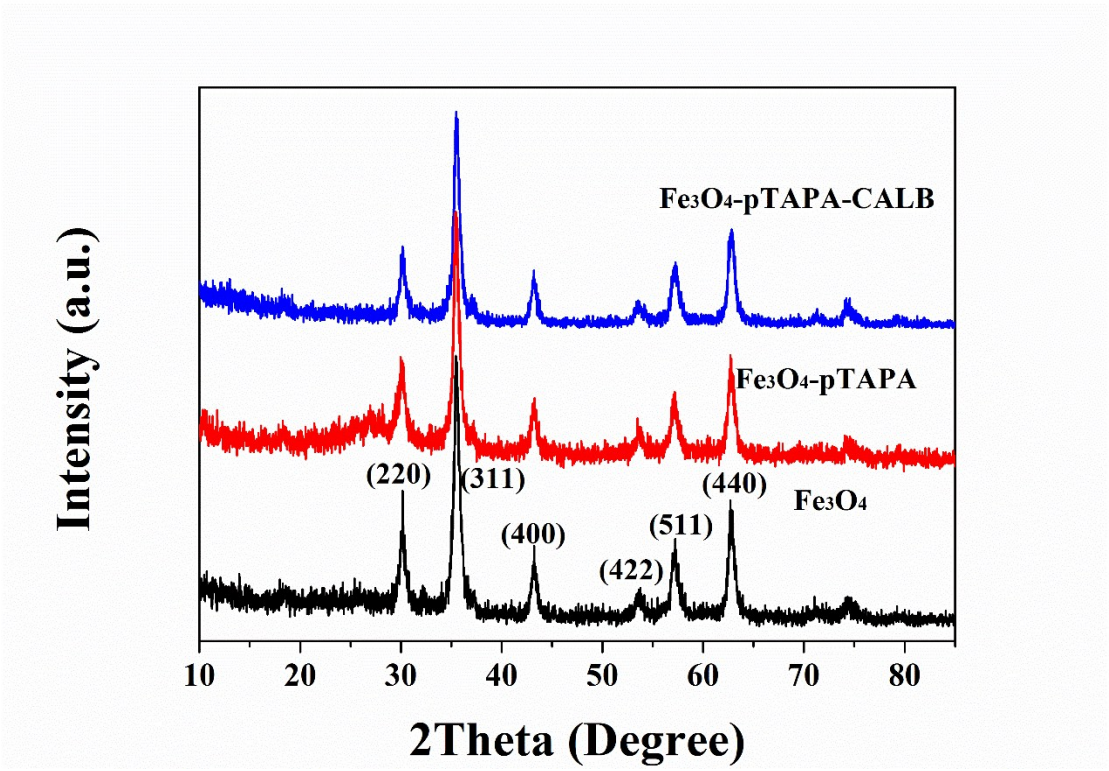

Fig. S6. XRD patterns of Fe_3O_4, Fe_3O_4-pTAPA and Fe_3O_4-pTAPA-CALB nanoparticles.

The crystal structures of all Fe_3O_4-based nanoparticles was investigated by powder X-ray diffraction (XRD). We can see both Fe_3O_4-pTAPA and Fe_3O_4-pTAPA-CALB nanoparticles had consistent peaks: (220), (311), (400), (422), (511), (440), which could be well indexed to the inverse index cubic spinel structure of Fe_3O_4 nanoparticles[4]. Notably, the XRD patterns of the Fe_3O_4, Fe_3O_4-pTAPA and Fe_3O_4-pTAPA-CALB nanoparticles exhibit similar features, which means that the crystal structure of the magnetite component was preserved during the whole synthesizing process and immobilization process.

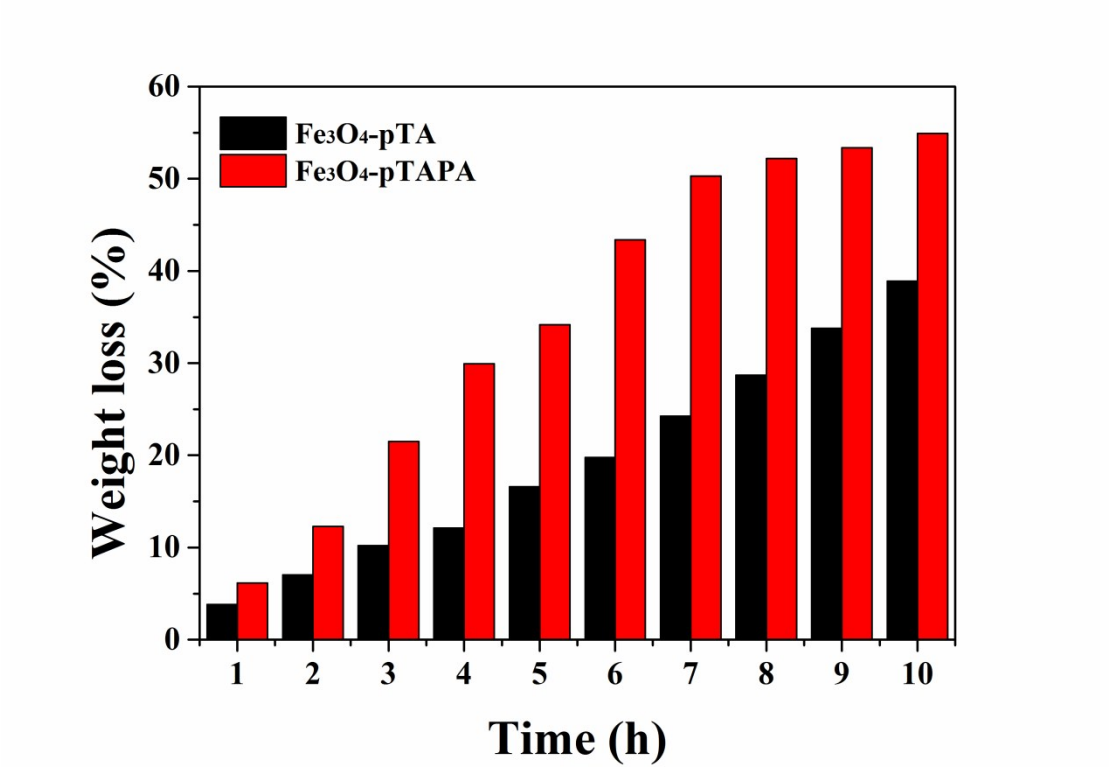

Fig. S7. The weight loss of pure TA or TA/TEPA binary system modified Fe_3O_4 nanoparticles at different polymerization time periods.

In order to clarify the presence of TEPA can accelerate the polymerization of TA, TGA analysis was performed to determine and compare the contents of polymerized pure TA or TA/TEPA binary system on Fe_3O_4 nanoparticles at different polymerization time periods. The results showed that the Fe_3O_4 nanoparticles modified by TA/TEPA binary system displayed more weight loss than those modified by pure TA at different time periods. These phenomenon can be explained by the fact that TA providing phenol groups and TEPA providing amino groups can fast form covalent bonds under weak alkaline conditions, and the formed pTAPA layer will strongly adhere on Fe_3O_4 nanoparticles by covalent and non-covalent interactions. This result significantly indicated that the presence of polyamine TEPA could accelerate the polymerization of TA on Fe_3O_4 nanoparticles.

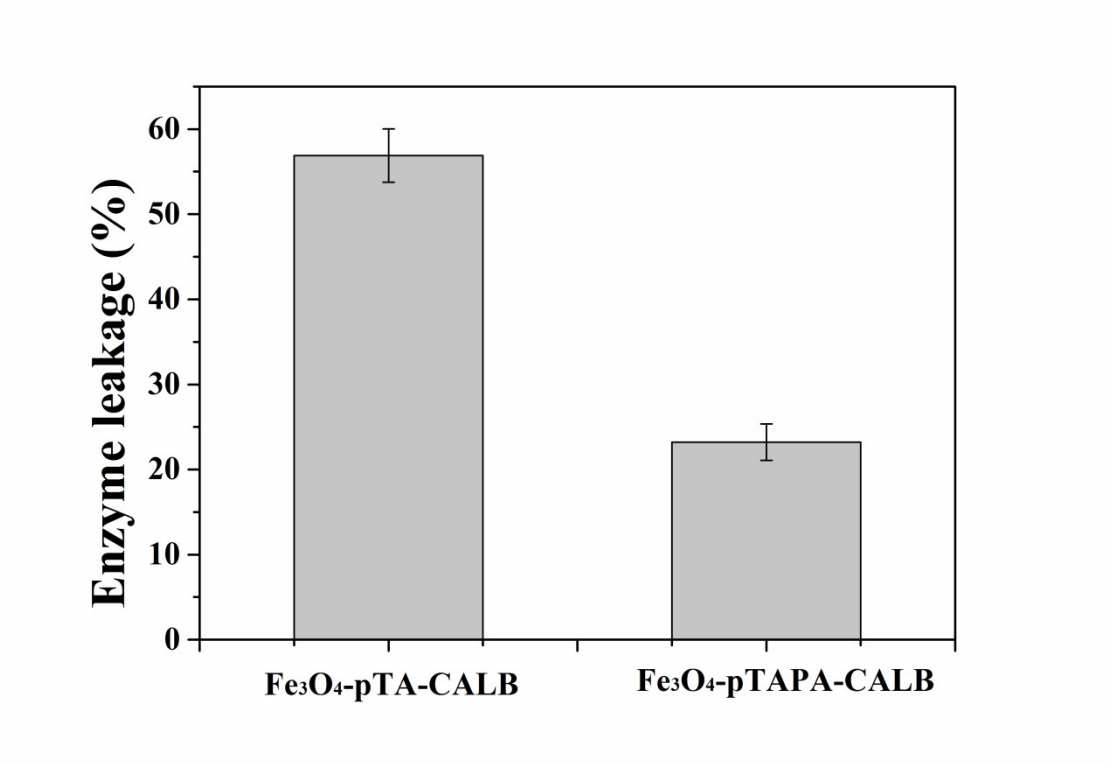

Fig. S8. The leakage profiles of CALB from Fe_3O_4-pTA-CALB and Fe_3O_4-pTAPA-CALB nanoparticles with stirring rate of 250 rpm for 7 days. Data are represented as mean ± SD (*n*= 3).

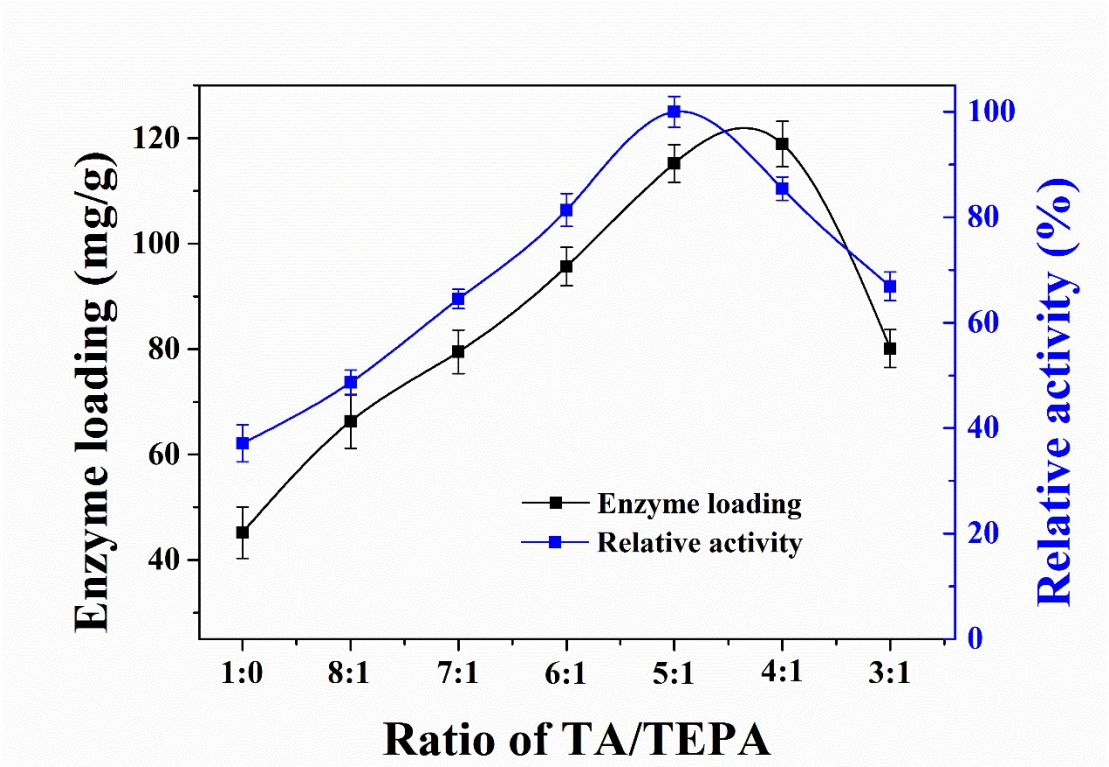

Fig. S9. The effect of TA/TEPA mass ratio on the loading capacity of Fe_3O_4-pTAPA nanoparticles (black line) and the relative activity of Fe_3O_4-pTAPA-CALB (blue line). Data are represented as mean ± SD (n = 3).

Fig. S9 exhibited that the loading capacity of Fe_3O_4-pTAPA nanoparticles was gradually increased when the TEPA at mass ratio of TA/TEPA was below 4:1, which might be due to the activated aldehyde groups increased with the TEPA concentration increased. After that, the enriched free aldehyde groups for enzyme immobilization will gradually be occupied by TEPA through covalent reaction, leading to decreased enzyme loading capacity. However, the relative activity of immobilized CALB began to decline when the TEPA at mass ratio of TA/TEPA was up to 5:1, which may be due to the space steric, mass transfer and diffusion resistance of supports[5]. Thus, considering enzyme loading and relative activity of immobilized CALB, the optimal mass ratio of TA/TEPA ratio was 5:1.

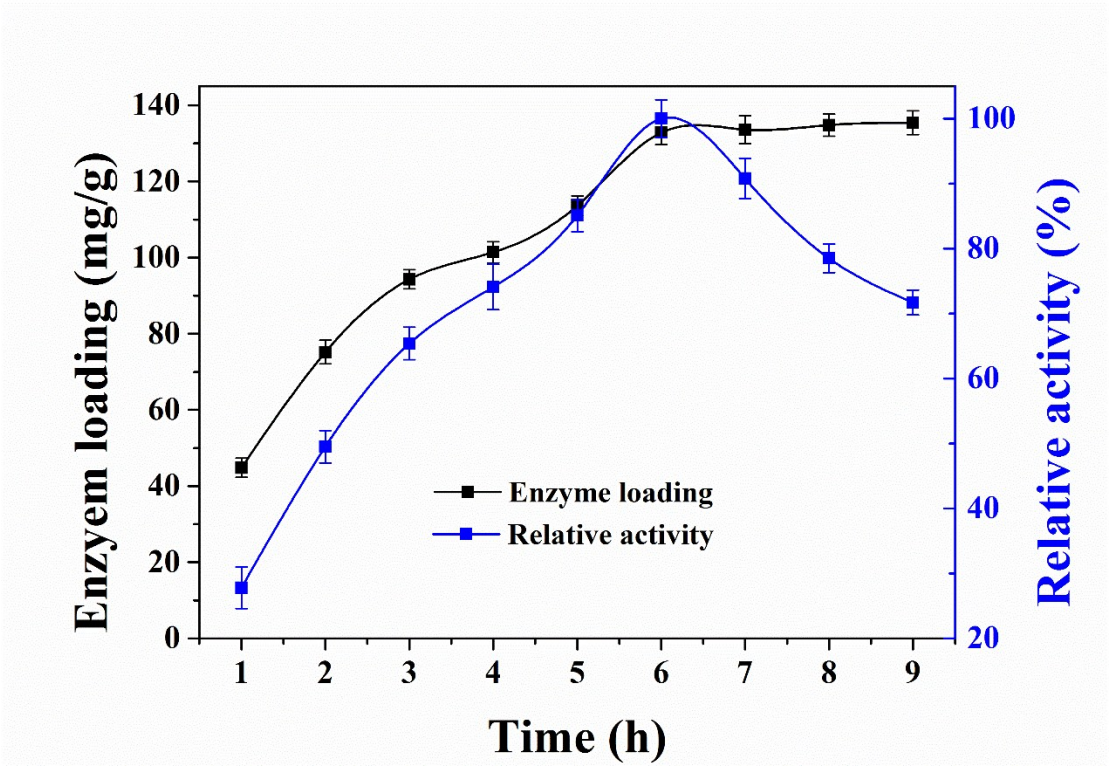

Fig. S10. The effect of immobilization time on the loading capacity of Fe_3O_4-pTAPA nanoparticles (black line) and the relative activity of Fe_3O_4-pTAPA-CALB (blue line). Data are represented as mean ± SD (n = 3).

Fig.S10 indicates the effects of immobilization on the loading capacity of Fe_3O_4-pTAPA nanoparticles and the relative activity of Fe_3O_4-pTAPA-CALB. The loading capacity increased with the increase of immobilization time. In contrast, the relative activity of immobilized CALB increased at the first 6 h and then decreased in the final 3 h. This finding may possibly because long-term shaking would cause denaturation of CALB in reaction system, further caused decreased activity. Hence, the most favorable immobilization time was 6 h.

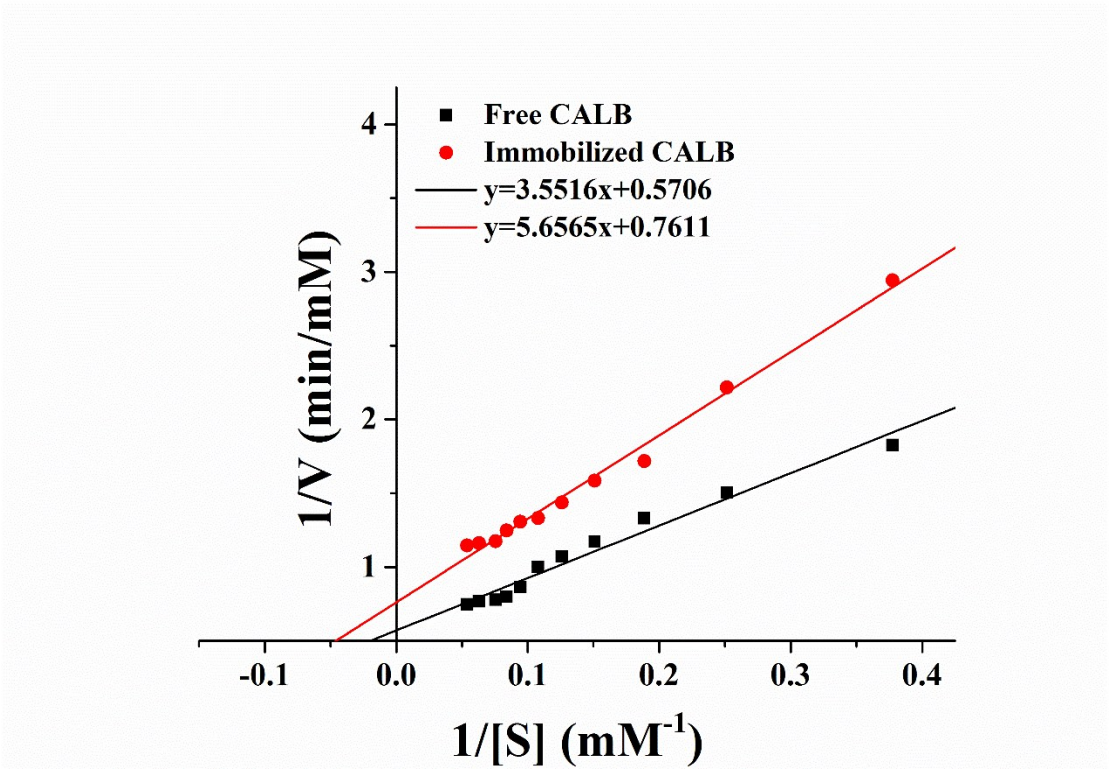

Fig. S11. The Lineweaver-Burk plots of free and immobilized CALB.

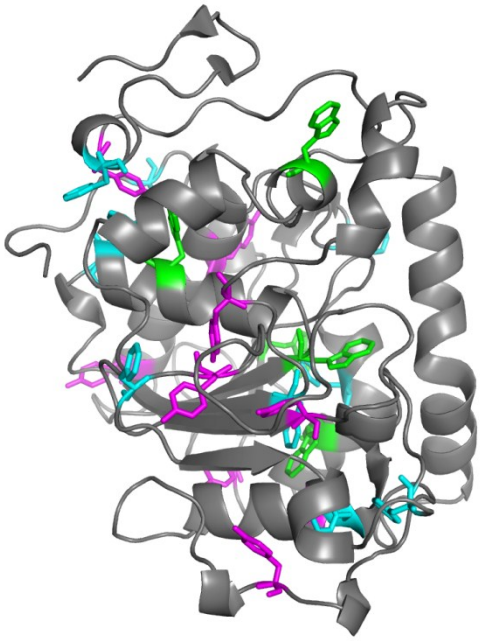

Fig. S12. The analysis of Trp, Tyr and Phe residues distribution in CALB (PDB ID: 1TCA). Green stick represents Trp, purple stick is Tyr and cyans stick is Phe.

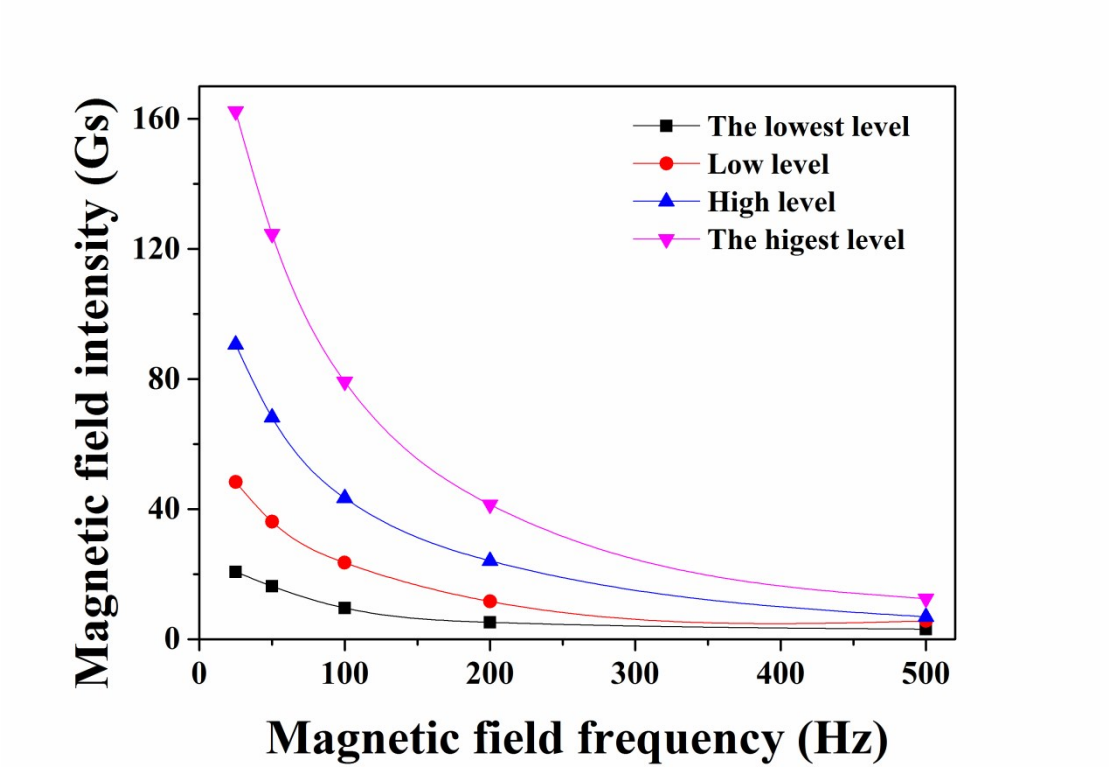

Fig. S13. Changes in measured magnetic field strength with frequency when the strength gauge was adjusted to four levels.

At each fixed level of strength gauge, the measured magnetic strength value decreased with the increase of magnetic field frequency. By adjusting the magnetic field strength and frequency on the control panel, the magnetic field strength measured at the center of coils could be operated from 2.8 to 162.3 Gs and the frequency could be adjusted from 25 to 500 Hz.

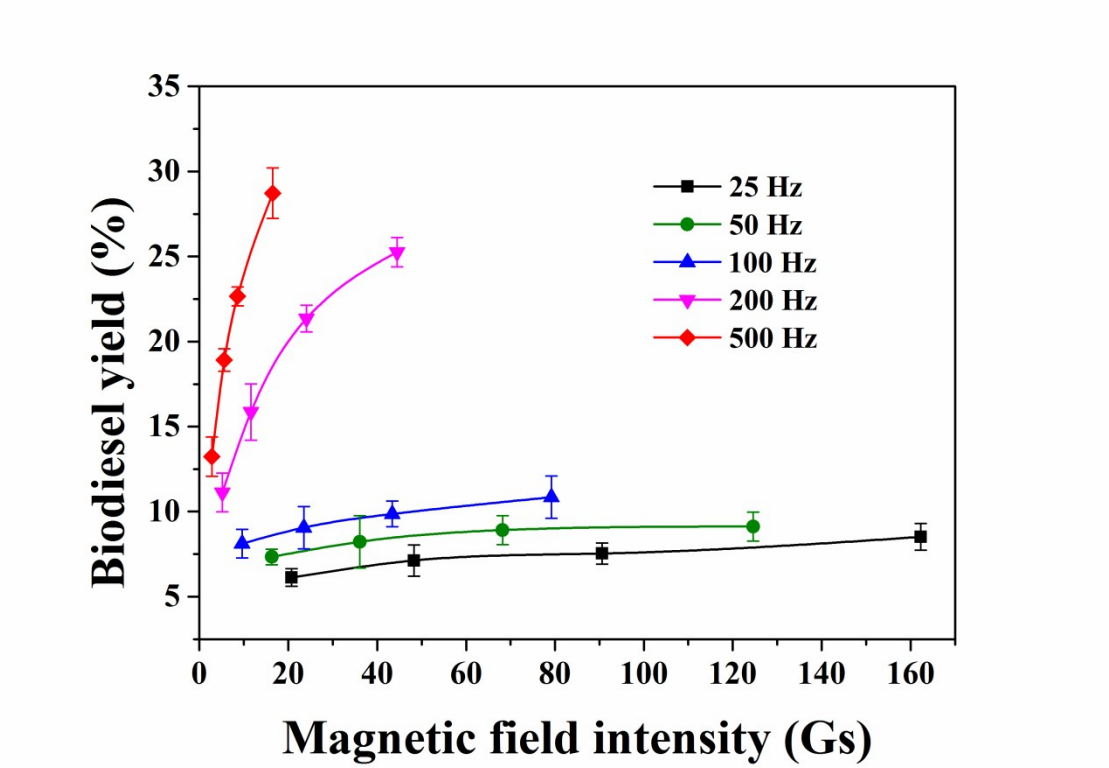

Fig. S14. The effects of alternating field strength and frequency on the biodiesel yield catalyzed by Fe_3O_4-pTAPA-CALB. Data are represented as mean ± SD (n = 3).

Table S1. The immobilization efficiency of different enzyme immobilization supports and specific activity of immobilized enzyme.

Samples	Amount of CALB added (mg/g)	Loading capacity (mg/g)	Immobilization efficiency (%)	Activity recovery (%)
Fe_3O_4-pTA	250	76.3	30.5	41.2
Fe_3O_4-pTAPA	250	132.8	53.1	56.7

Table S2. Secondary fractions of CALB before and after immobilization calculated from CD spectra[a].

Sample	H(r)	H(d)	S(r)	S(d)	Trn	Unrd
Free CALB	0.198	0.314	0	0.086	0.120	0.281
Fe_3O_4-pTAPA-CALB	0.013	0.223	0	0.054	0.287	0.423

[a]H(r): regular α-helix, H(d): distorted α-helix, S(r): regular β-sheet, S(d): distorted β-sheet, Trn: turn, and Unrd: unordered.

Reference

1. A. Yu, Y. Wang, E. Barlow and F. Caruso, *Advanced Materials*, 2005, **17**, 1737-1741.
2. D. Yang, X. Wang, J. Shi, X. Wang, S. Zhang, P. Han and Z. Jiang, *Biochemical Engineering Journal*, 2016, **105**, 273-280.
3. G. Cheng, M.-D. Zhou and S.-Y. Zheng, *ACS Applied Materials & Interfaces*, 2014, **6**, 12719-12728.
4. C. Hou, Z. Qi and H. Zhu, *Colloids and Surfaces B: Biointerfaces*, 2015, **128**, 544-551.
5. T.-T. Xia, C.-Z. Liu, J.-H. Hu and C. Guo, *Chemical Engineering Journal*, 2016, **295**, 201-206.